Aircraft Design Final Report

Flight Simulation of *Brett the Jet*

MMAE 414 - Fall 2019

Mikel Woo
Benjamin Thrun
Hasan Swain
Sardor Nazarov
Kevin Hildreth
Zachary Bonson

Table of Contents

1 Executive Summary

This report contains the solution to the flight simulations of the midterm aircraft design. Utilizing *Brett the Jet* from the midterm, aircraft stability and control derivatives were solved for using XLFR5. Upon solving for the stability and control derivatives, a Simulink model was developed which satisfies three distinct objectives. The objectives that were achieved are a takeoff and climb performance, hold performance and landing performance. The results from these three conditions satisfies the requirements outlined in the objectives for this project.

2 Aerodynamic Data

2.1 Aircraft Control Derivatives

Accurately simulating the flight dynamics of the aircraft required obtaining the force and moment coefficients as they change with angle of attack (α), sideslip (β), and control inputs. All of the coefficients are dependent upon angle of attack. Lift, drag, and pitching moment are additionally dependent upon the elevator deflection angle (δ_e). The effects of sideslip and the other controls is negligible. Conversely, heave force, rolling moment, and yawing moment are dependent on sideslip angle, airleron deflection (δ_a), and rudder deflection (δ_r).

Obtaining this data began with running XFLR5 simulations of the aircraft with different control inputs. The analysis was performed over a range of angles of attack and sideslip angles for each configuration. Figures A.1a-A.1l show the data collected.

3 Takeoff and Climb

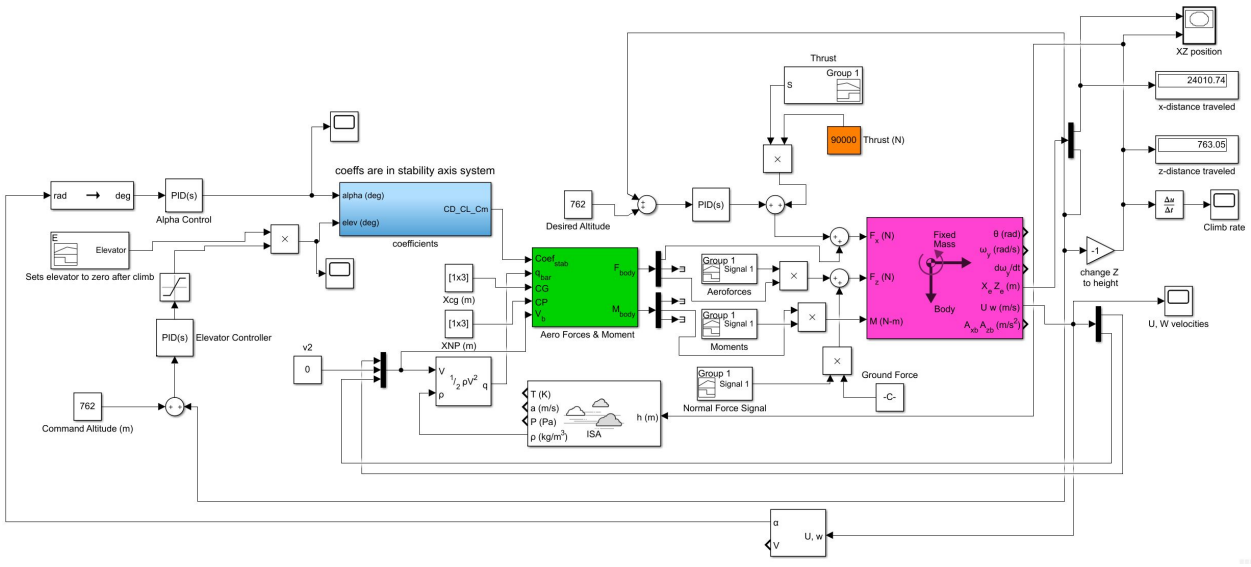

Figure 3.1: Block diagram for takeoff and climb portion of simulation

3.1 Command Trajectory vs. Simulation Prediction

The aircraft begins from rest at 0 m/s and accelerates to a takeoff speed of 90 m/s over 40 seconds. At this time, the aircraft lifts off the ground and begins to climb to the holding altitude of 762 m (2,500 ft). Upon reaching the desired altitude, the aircraft levels and maintains steady, level flight for 20 seconds.

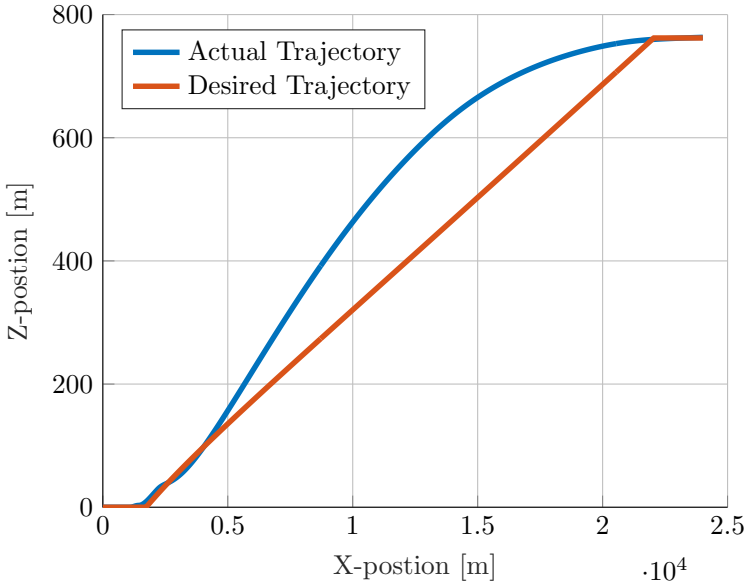

Figure 3.2: Trajectory of aircraft during takeoff and climb

To achieve this performance, the aircraft was controlled via altitude feedback control in Simulink. The code creates an error value that shows the difference between the actual altitude and the desired altitude. That is then fed into a PID controller that corrects the units of the feedback signal to the correct order of magnitude to be fed back into our elevator deflection input. The gains were set to both correct the units and ensure that if the aircraft needed an increase in altitude, the elevator would deflect upward, and vice versa. The saturation block on the elevator control loop is to give the physical restriction of the elevator deflection angle. The elevator may not exceed +/-20°, and the saturation block simulates that physical limitation. There is a signal builder block that gradually starts to set the elevator deflection back to zero after the climb phase. This is to simulate a pilot leveling out the aircraft, and is one of the factors that allows the aircraft to level off and stay flying level after the climb phase. The angle of attack feedback comes from the *incidence* block in Simulink that takes U and w velocity as an input and provides the angle of attack as an output. This output was converted from radians to degrees and then fed into a PD controller to give control over the angle of attack. Altitude feedback for thrust was also utilized to help the aircraft achieve this level flight. More will be said on these pieces of control in subsequent sections of this report.

The signal builder blocks leading into the *3DOF* block serve to simulate the normal force the ground exerts on the aircraft while it is on the ground, and give a ramp start to the aerodynamic forces and moments simulation until the aircraft is up to the speed of takeoff. This means that initially the aerodynamic forces and moments have no effect, because the aircraft is at rest, and then ramp up to full functionality of a moving aircraft. This is beneficial because the aircraft may then accelerate down the runway without being unrealistically influenced by the simulation of aerodynamic forces and moments.

3.2 Climb Rate

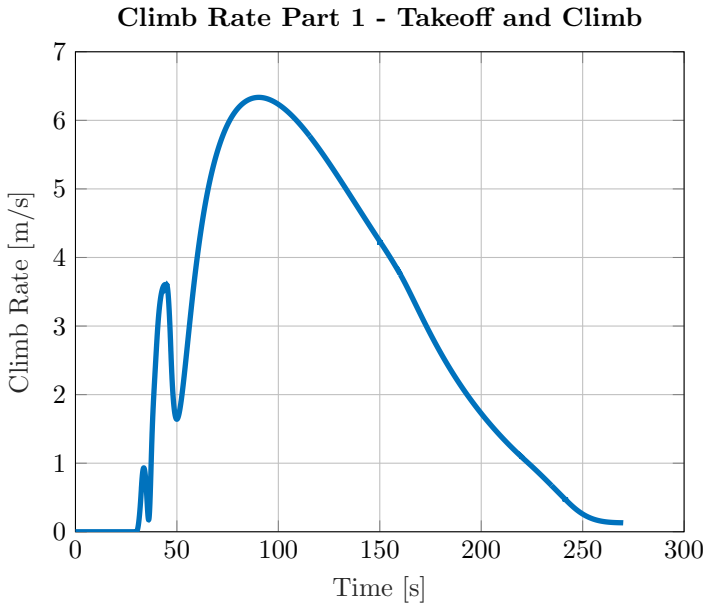

Figure 3.3: Climb rate during takeoff and climb

In this section we see the plot of the climb rate of our aircraft over the 270 second duration of the takeoff/climb simulation. We see for the initial 40 second, the climb rate is zero. This is in line with what we hope and expect as in that time the aircraft is accelerating down the runway, and not increasing altitude yet. After takeoff at 40 seconds, our ideal case is a rapid increase to a 5 m/s climb (equivalent to a 1000 ft/min climb). We see our climb rate however depict an *average* climb rate of 5.08 m/s. This climb rate is calculated on average from the change in altitude, 762 meters, over the time of climb, 150 seconds. The climb rate behaviour is due to our decision to utilize altitude feedback rather than rate feedback. If we had used rate feedback, this value would be easier to set at a constant. We decided to trade this behaviour for better performance in our other parameters, however, and maintain an average climb rate of 5.08 m/s (1000 ft/min) as directed in the requirement. The decision to utilize altitude feedback allowed us to more readily control the ability of the aircraft to level out at the end of the climb.

3.3 Reaching Altitude and Level Flight

As we see in Figure 3.3, our aircraft levels out after the climb phase, and maintains level flight for 20 seconds. This characteristic was accomplished via the feedback and control of the aircraft altitude. This feedback decision allowed us to give the code an easy method of setting to the aircraft to trim after the climb phase, as the error goes to zero when the aircraft reaches the desired altitude. This is why we see our elevator deflection go to zero and the angle of attack go to trim in Figures 3.6 and 3.5 respectively. This yields a smooth leveling of the aircraft after climb. As shown in 3.3, the aircraft maintains altitude for the required 20 seconds after leveling. Another crucial component to achieving level flight after the climb was altitude feedback to control the thrust of the aircraft.

3.4 Thrust

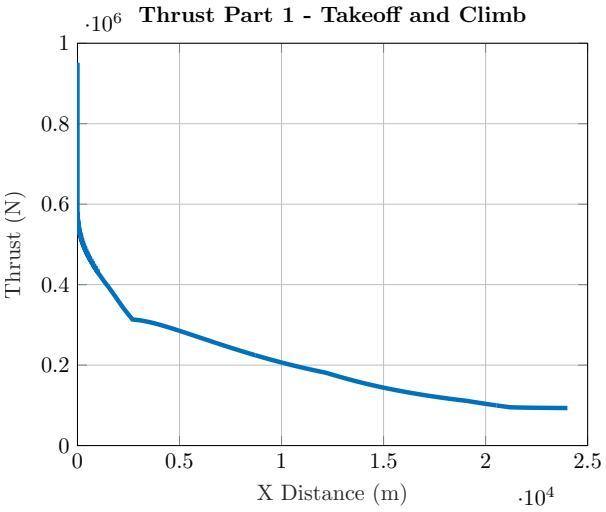

Figure 3.4: Thrust during takeoff and climb as a function of horizontal position

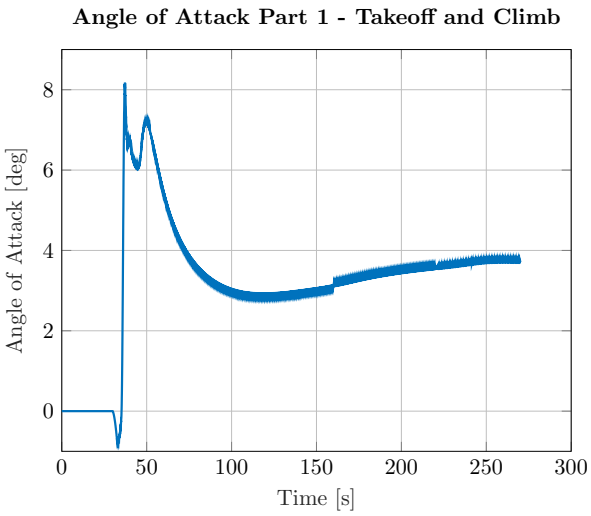

Figure 3.5: Angle of attack during takeoff and climb as a function of time

The thrust was varied via an altitude feedback loop. The loop is essentially adding thrust to the baseline of 90,000 N until we reach altitude, at which point the thrust remains at 90,000 N. This value was chosen as the baseline because that is the trust we found necessary for our aircraft to maintain level flight at 762 m (2500 ft). Hence, the aircraft thrust is decreasing as it increases in altitude, starting at a maximum value of 550,000 N, which is below the maximum value that our combined two Rolls Royce Trent 800 engines can produce, which is 840,000 N [3].

3.5 Angle of Attack

The angle of attack of the aircraft is not to exceed 15°, and as we can see in Figure 3.5 the simulator predicts a maximum angle of attack of 8°, thus satisfying the requirement. This maximum angle of attack is at lift-off, which makes sense given that takeoff will require a great initial lift. This result coincides with our climb rate and elevator deflection plots as all three indicate an initial high rate of climb and then a decrease. One area of this plot that does not make sense, and is somewhat concerning, is that the angle of attack briefly goes negative right before takeoff, and then jumps rapidly up, which could be catastrophic, depending on the airfoil. The value of the angle of attack is between -0.5° and -1°, and thus with a cambered airfoil we can still expect the lift to be positive here. This means that we can expect this aircraft to still be capable of taking off, as it does utilize a cambered NASA SC(2)-0714 airfoil [4]. Overall this plot is reasonable for a takeoff, as our angle of attack (after an initial drop) starts positive does not get too high, and decreases over time to move closer to the trim condition as the aircraft climbs and levels off at altitude while not dropping below zero angle of attack.

3.6 Elevator Deflection

The geometric limit of our elevator control surface is such that the elevator may not exceed +/-20°, and as Figure 3.6 shows, the minimum elevator deflection is -4.5°, and the maximum is 0.5°. The initial negative elevator deflection is valid as a negative elevator deflection is one that pushes the trailing edge up, which in turn pushes the nose of the aircraft up, thus increasing the angle of attack. This is good behaviour for our elevator as we want the angle of attack to increase in takeoff. The change to a positive elevator deflection is another indicator that the aircraft is approaching trim, as the control surface becomes a stabilizing agent at this point. The elevator deflection then decays to zero, which is good as we hope for this to happen as we level off and wish our angle of attack to reach a constant, level value.

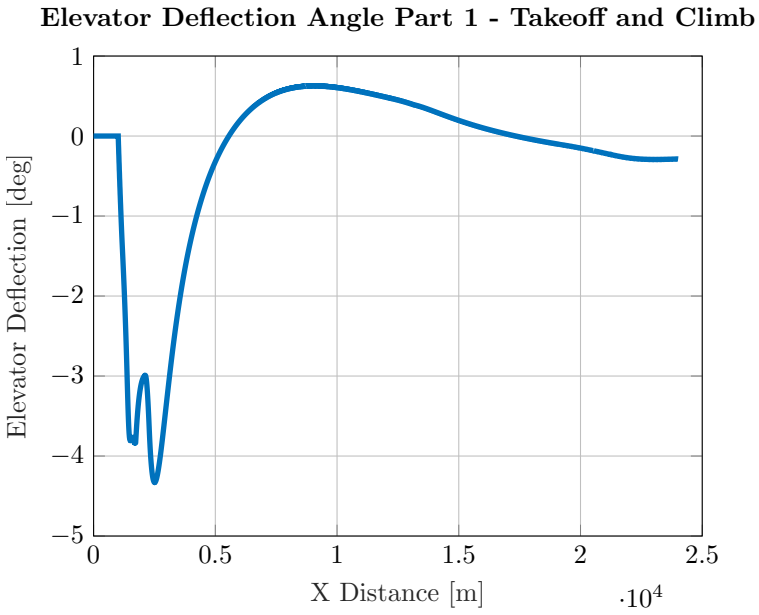

Figure 3.6: Elevator deflection during takeoff and climb as a function of horizontal position

4 Holding Pattern

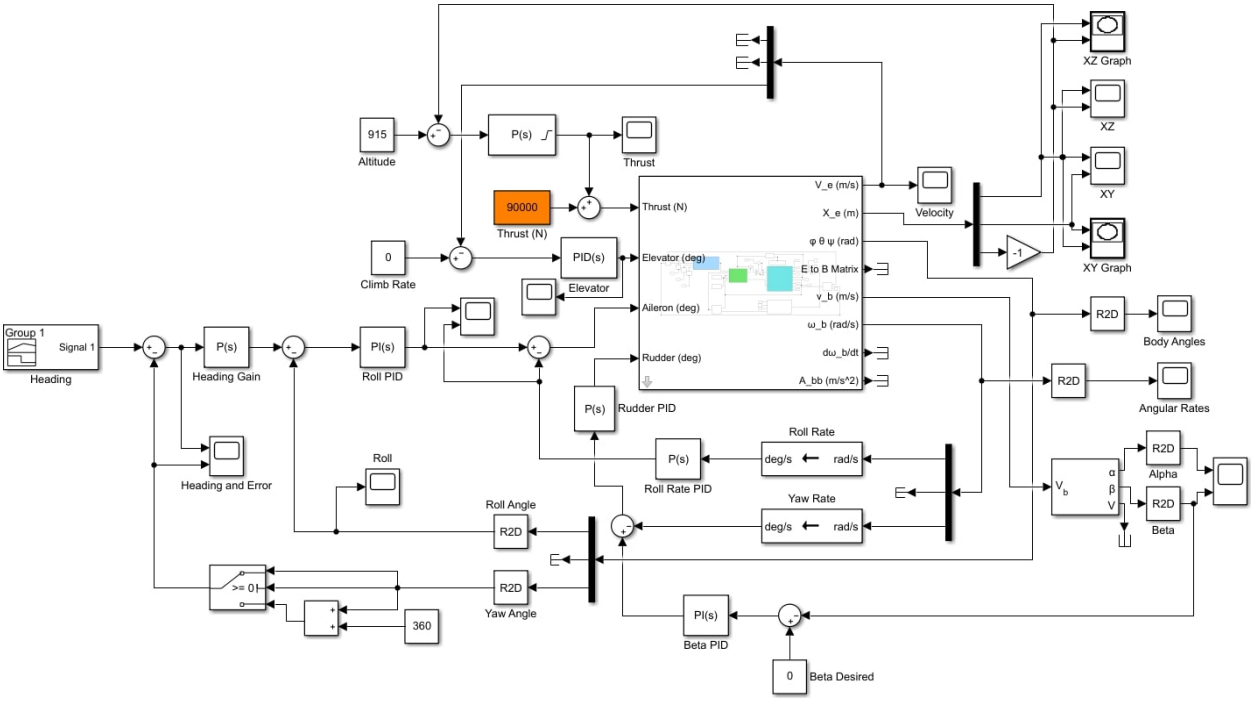

Figure 4.1: Simulink Model of Holding Pattern Controller

4.1 Commanded Trajectory vs. Simulation Prediction

The holding pattern consists of the aircraft maintaining heading until reaching the heading fix. At this point the aircraft begins a turn at a rate of 3 °/s to the outbound leg. This turn is continued for one minute until the aircraft has turned 180°. The aircraft maintains this heading for another minute before beginning another 180° turn at the same rate. Upon reaching the original heading, the aircraft will reach the holding fix after a minute. For the specified mission profile, the aircraft shall perform the maneuver at 3,000 ft (∼915 m) and 175 kts (∼90 m/s).

The simulation was achieved through roll, yaw, altitude, and thrust control. Using the six degree of freedom block, a controller was designed to provide a solution to the holding pattern. A full depiction of the Simulink model can be seen in figure 4.1. The final plot of the flight path vs. desired holding pattern can be observed in figure 4.2. The difference between the trajectory and actual holding pattern can be attributed to the model speeding up a small increment to maintain lift, which subsequently increases the turn radius and leads to the discrepancy that is observed in figure 4.2.

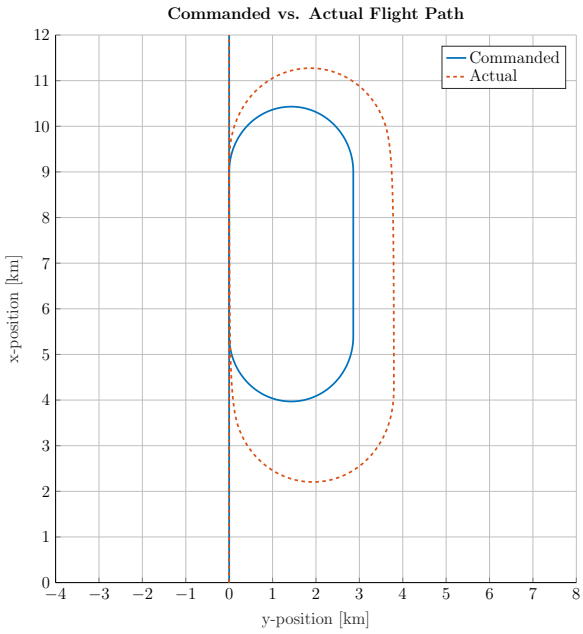

Figure 4.2: Desired vs. Actual Holding Pattern

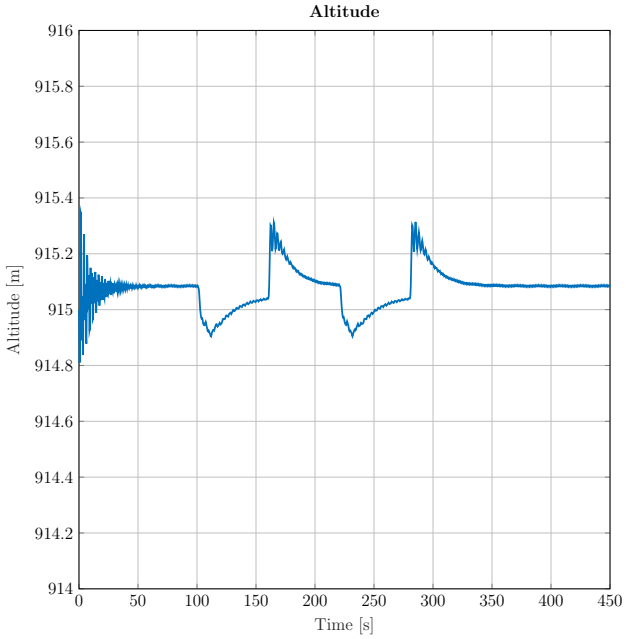

Figure 4.3: Altitude of Holding Pattern

4.2 Heading

Heading was controlled through a combination of roll and roll rate. A determination of the necessary roll angle is determined through the error of the current heading and desired heading. The determined roll angle is then compared to the current roll angle to get a required aileron input. However, to prevent unstable or jittery behavior an extra part was added to try and keep the roll rate at zero. The combination of these results in an aileron deflection angle to reach the desired heading. The desired heading is generated through a *Signal Builder* block to reach a heading of 180° after 60 seconds and then maintain that heading for another 60 seconds. This is done for each leg of the holding pattern. The resulting roll angle can be seen in figure 4.6.

4.3 Altitude

Altitude was controlled through variation in thrust. The error was taken and fed through a proportional controller and limited to the thrust range of the engine mentioned earlier. This was then added to a baseline thrust that acts as the thrust at the cruise. Figure 4.3 shows that there are very negligible changes in altitude. However, it does contain oscillations which can be attributed to the controller only using proportional gains.

4.4 Sideslip

An important aspect of making turns is ensuring they remain coordinated. Both to maintain passenger comfort and prevent any undue aerodynamic effects (such as stalling the outboard wing). Rudder control was used to correct for changes in sideslip to maintain a coordinated turn. The controller takes the current sideslip angle and determines how much rudder input is required to bring it back to zero. This output is then subtracted from the yaw rate to induce some damping. The sideslip angle over time is shown in figure 4.4. It can be seen that the angle never breaches two degrees. Staying within a small boundary and thus is coordinated.

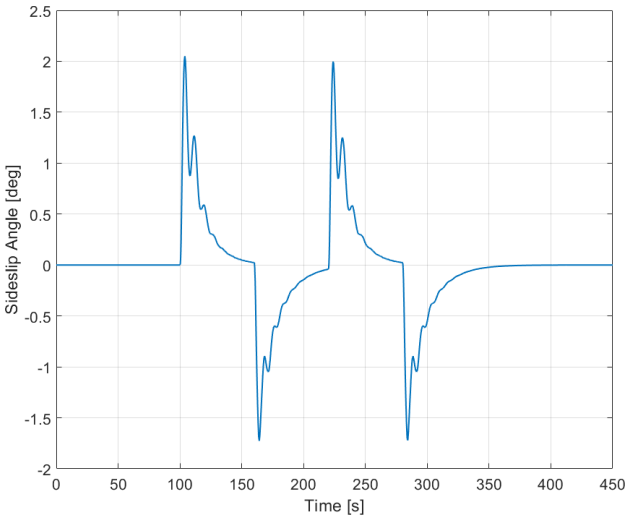

Figure 4.4: Sideslip Angle

4.5 Flight Speed

Figure 4.5 demonstrates the total velocity of the aircraft in the X and Z direction. The velocity hovers between 90 and 95 m/s. This is ideal since, in the mission statement for the holding pattern, 175 kts (∼90 m/s) is what is desired. Velocity is maintained as a result of the thrust control.

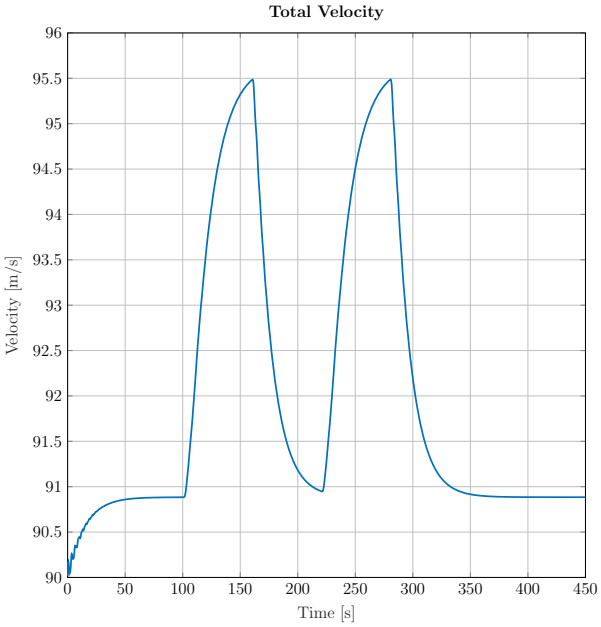

Figure 4.5: Velocity of Aircraft

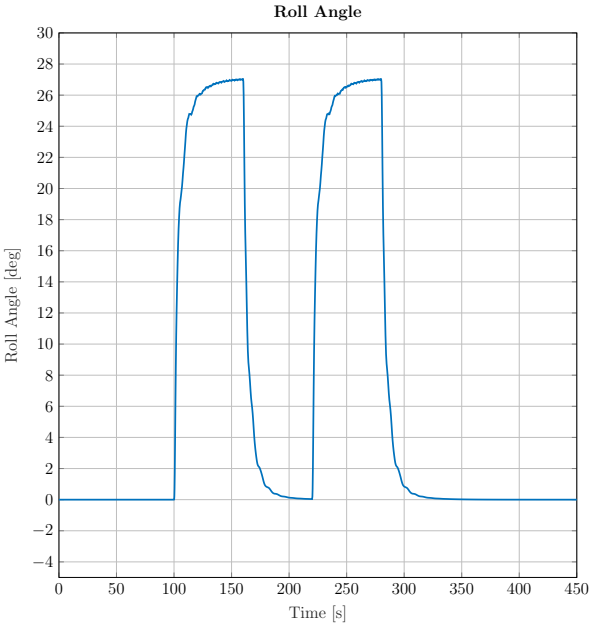

Figure 4.6: Roll Angle

5 Descent and Landing

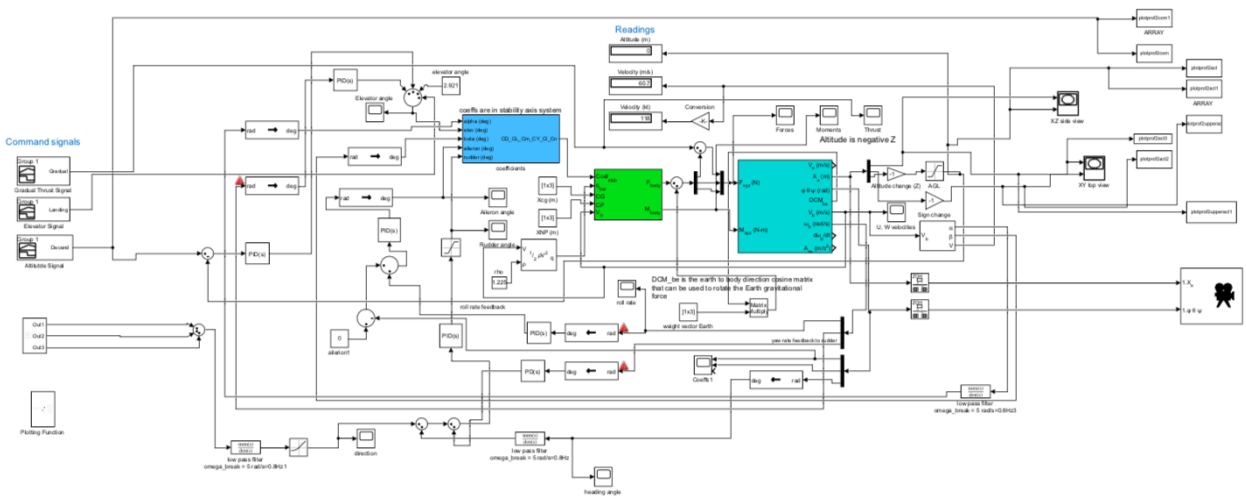

Figure 5.1: Landing Schematics

5.1 Command Trajectory vs. Simulation Prediction

In the last part of the simulation, our aircraft had to perform descent and landing maneuvers according to the requirements specified. It has been stated that the aircraft starts descending at an altitude of 1000 ft., which is equivalent to 304 meters as depicted on the graphs. Our aircraft enters the downwind leg of a left-hand landing at 45°, and the speed does not exceed 175 kts. When the altitude drops to 600 ft (180 m.), the speed also decreases to 150 kts. When the airplane performs the last left turn at 90°, the speedometer shows 140 kts., which is in compliance with the objectives. Finally, the path aligns with the runway at landing.

As it can be observed from the plots, the actual and commanded paths for both the side and top views are relatively close to each other. There is a little deviation caused due to a manual variation of commanded thrust values, which was necessary to control the speed at different altitudes.

We know that landing is mainly performed using longitudinal and lateral direction planes, hence, the aerodynamic coefficients, stability and control derivatives were implemented from xflr5 in order to model the actual trajectory. 6 DOF block was used to transform forces and moments from the body to Earth axis. The aerodynamic coefficients are obtained by interpolating angles and deflections.

We have used control blocks that send signals to the rudder, elevators and ailerons to perform turns. The 45° had a step input of 150 seconds, -90° at 750 seconds, and 90° at 1250 seconds. A low pass filter was also necessary to be included in order to control the behavior of the turns. The PID controller was responsible for diminishing the oscillations. The coefficients were selected based on a trial and error method. Therefore, there are still some oscillations present on the graphs. The overall descend and landing last for about 2800 seconds.

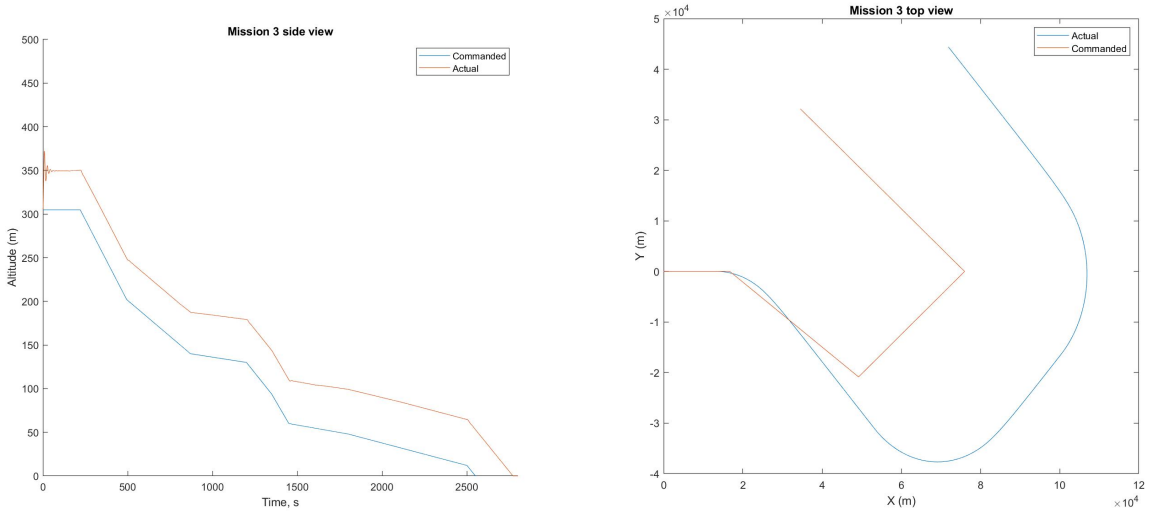

(a) Side View **(b)** Top View

Figure 5.2: Approach and Landing Views

5.2 Aileron Input

The aileron control system consists of a roll angle feedback, commanded signal builder, and a roll rate feedback. The primary task of the signal builder is to send a desired aileron angle, and after that the roll angle feedback is subtracted from the input so that it returns to a zero bank angle. We have set up the aileron angle input command from the signal builder, because a manual input to the ailerons is what most aircraft manufacturers implement. A plot of aileron angle deflection vs. time is represented in Figure 5.3

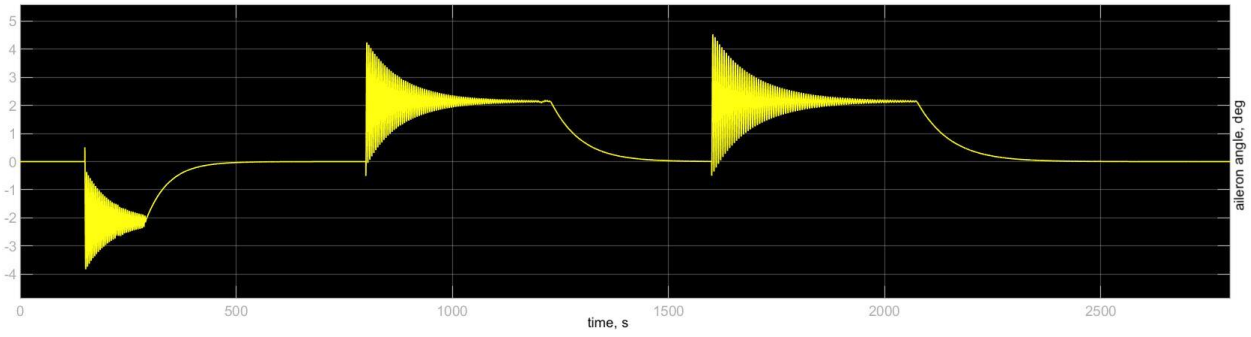

Figure 5.3: Aileron angle vs. Time

5.3 Rudder Input

The rudder control, in its turn, consists of the PID controller attached to the commanded heading angle and yaw angle feedback. To prevent yaw rate error, it is summed with an inner loop yaw rate feedback. To avoid any overshoots, the rudder angle command block was connected to a saturation block. It can

be observed from Figure 5.4 that the rudder angle range was from -15° to +15°, and it is in compliance with the time at which turns were actually taking place.

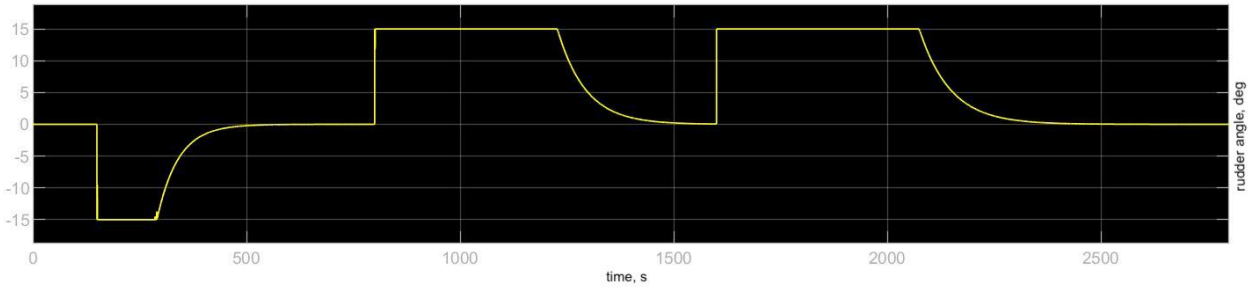

Figure 5.4: Rudder angle vs. Time

5.4 Thrust Input

In order to be able to meet speed requirements at given altitudes, the thrust input had to be adjusted manually from the thrust command signal block. Therefore, it was decided that the thrust switch was not necessary. We have used a gradual mode to perform the mission. The thrust was gradually reduced to 0 N at a final 90° turn.

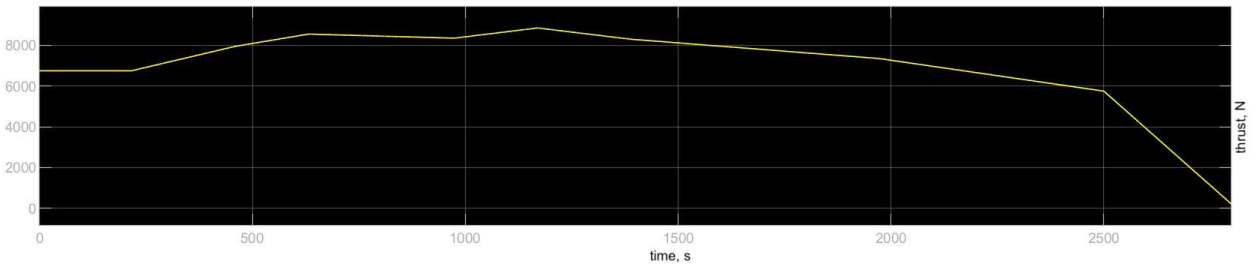

Figure 5.5: Thrust input vs. Time

5.5 Bank Angle

The bank angle meets the requirements of not exceeding a 60° limit. The bank angle is achieved by increasing lift on one wing while decreasing it on the other one. The reason why the angle is so small is that we were primarily relying on the rudder to perform turns. The maximum bank angle that our aircraft experiences is 2.5°. The Figure 5.6 shows the angle variation versus time. It can be seen that there are some oscillations on this graph as well. To reduce that, one has to vary the PID controller constants. However, this is the best result that we could achieve.

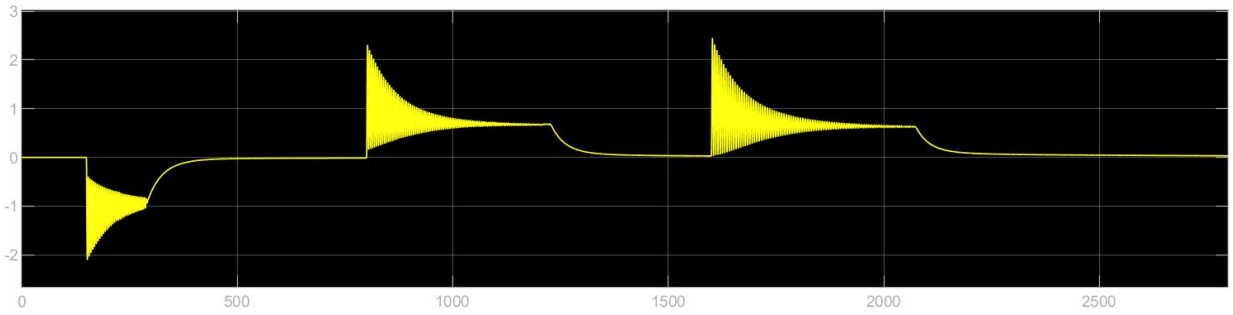

Figure 5.6: Bank angle vs. Time

6 Conclusion

The team's simulation for the three flight conditions, takeoff and climb, holding pattern, descent and landing were satisfied. Using *Brett The Jet* as the model aircraft; control derivatives were solved for using XFLR5 and were utilized when solving for the three flight conditions in Simulink. The solution demonstrated that the team's work may not be perfectly identical to the trajectory, however it is a very close approximation that is satisfactory.The difference in the trajectory vs. actual can be attributed to climb rate not being fed back, instead altitude is fed back and since climb rate varies slightly the graphs do not line up perfectly. For the holding pattern, there is deviation due to the aircraft speeding up to maintain lift which increases the turn radius slightly. The difference for descent, is from a manual variation of commanded thrust. With this solution the team has a better understanding of how the aircraft maneuvers, and the thought processes that go into setting up the Simulink model to solve for the three distinctive flight conditions. The mission requirements were achieved and the simulations provided insightful knowledge to the aircraft.

References

[1] Yechout, Thomas R., et al. *Introduction to Aircraft Flight Mechanics*. 1st ed., AIAA, 2014.

[2] Raymer, Daniel. *Aircraft Design: A Conceptual Approach*. 6th ed., AIAA, 2018.

[3] Rolls Royce Trent Series (n.d.). Retrieved from www.rolls-royce.com

[4] Fasoro, Kelley, Ott, Thrun, Writenour. *MMAE 414: Aircraft Flight Design: High Capacity Short Range Transport Aircraft Design Proposal*, 2019.

A Coefficients

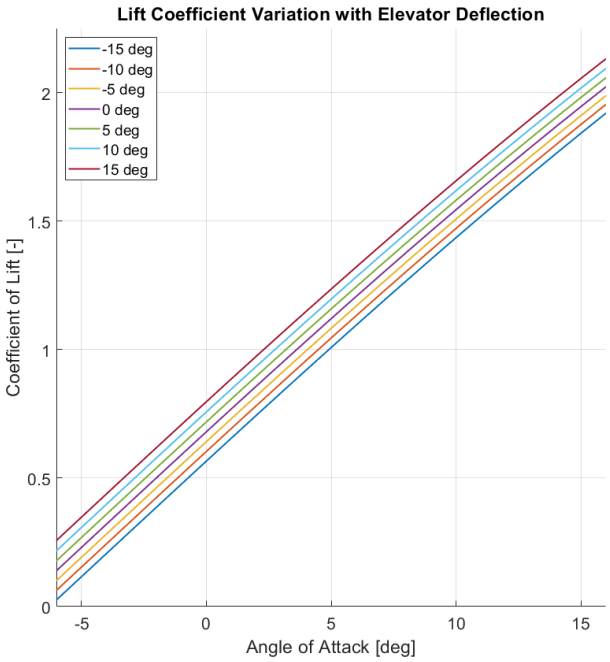

(a) Lift Coefficient with Changes in δ_e

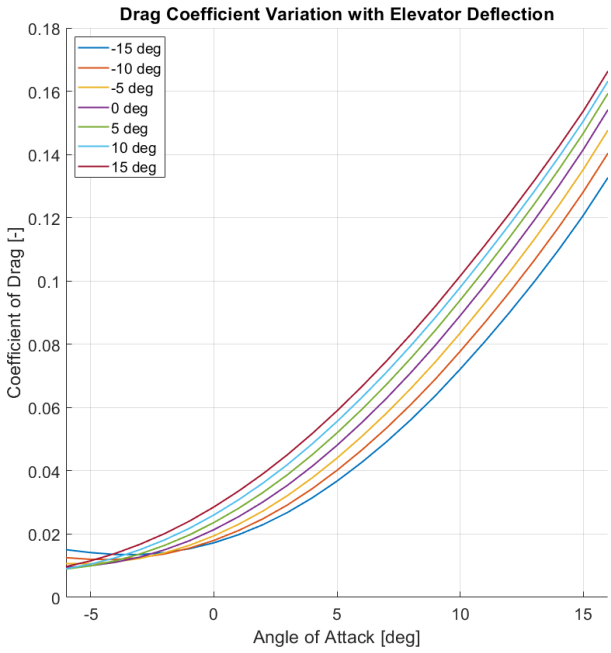

(b) Drag Coefficient with Changes in δ_e

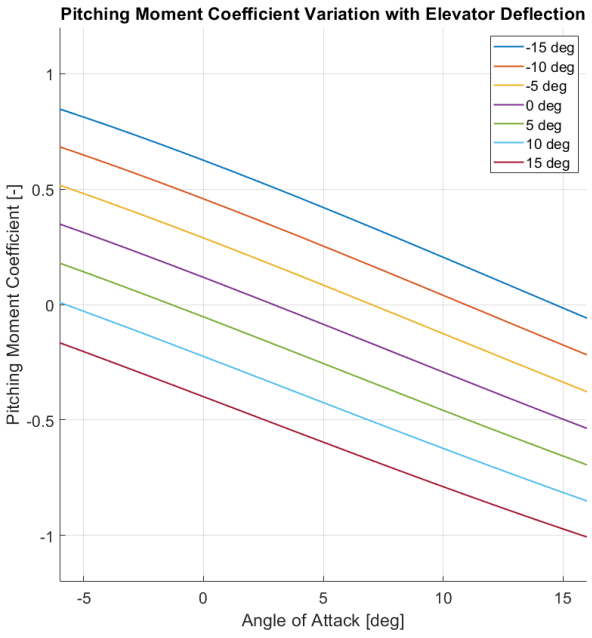

(c) Pitching Moment Coefficient with Changes in δ_e

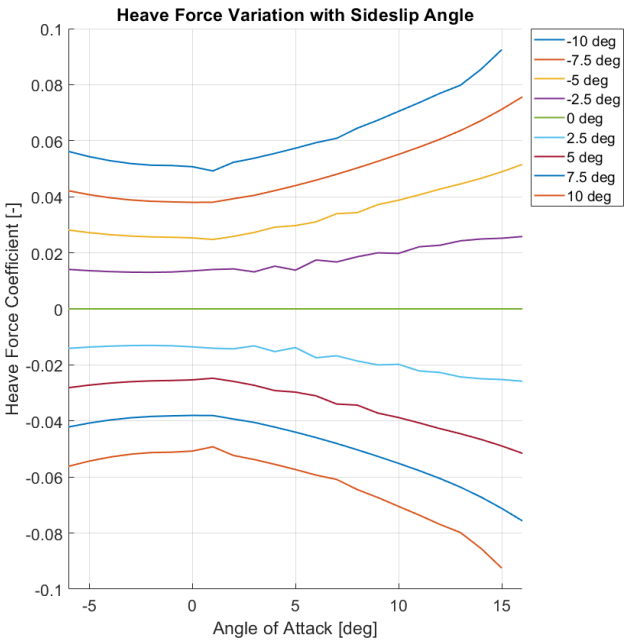

(d) Heave Force Coefficient with Changes in β

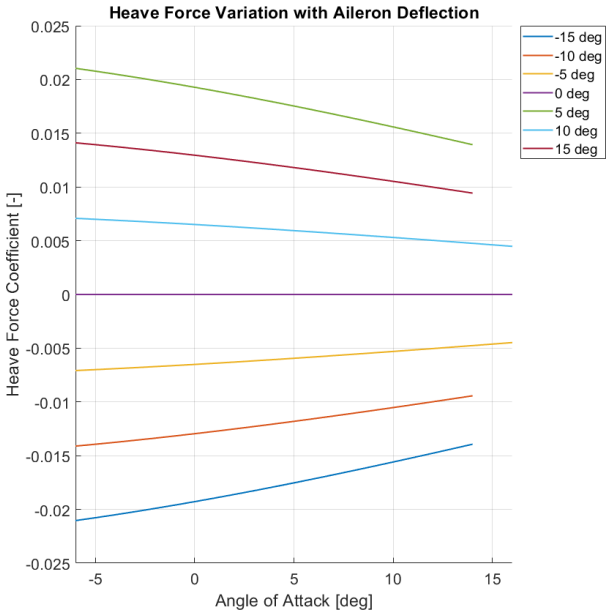

(e) Heave Force Coefficient with Changes in δ_a

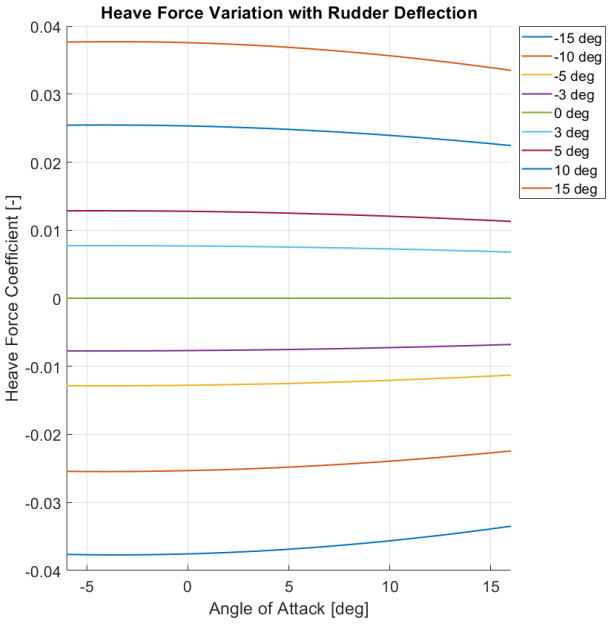

(f) Heave Force Coefficient with Changes in δ_r

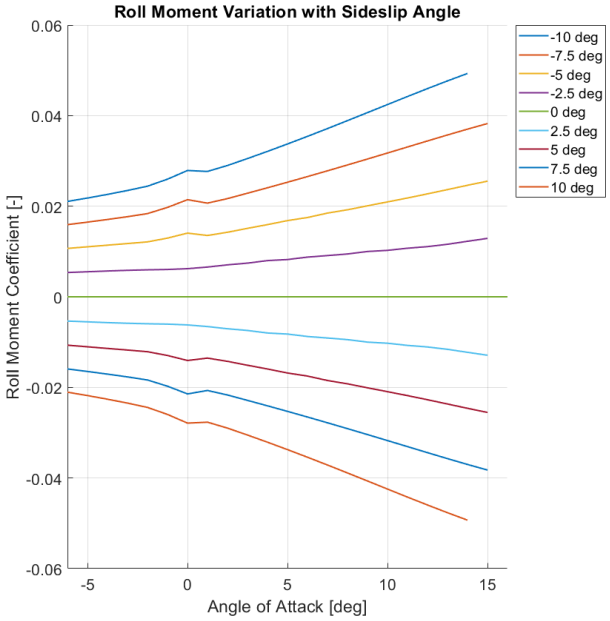

(g) Roll Moment Coefficient with Changes in β

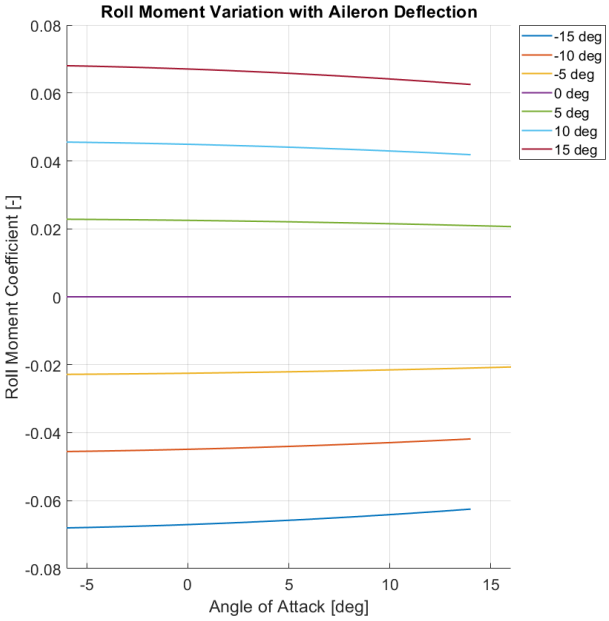

(h) Roll Moment Coefficient with Changes in δ_a

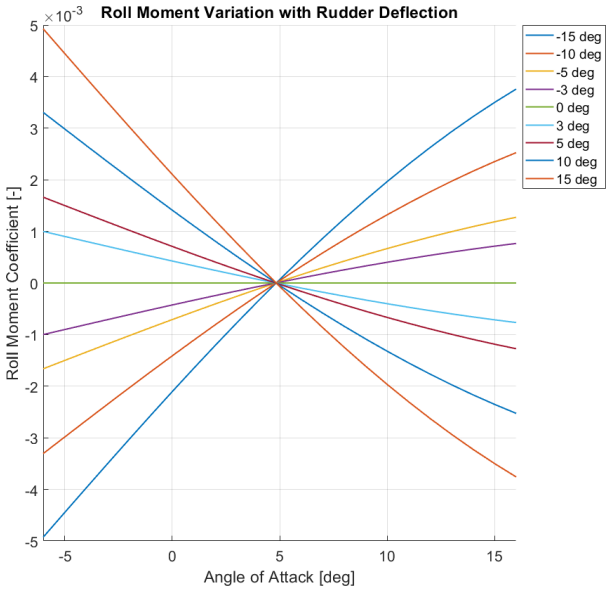

(i) Roll Moment Coefficient with Changes in δ_r

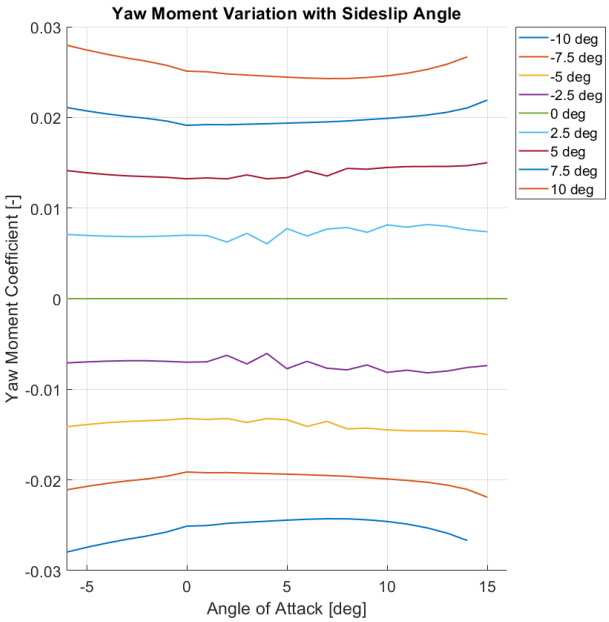

(j) Yaw Moment Coefficient with Changes in β

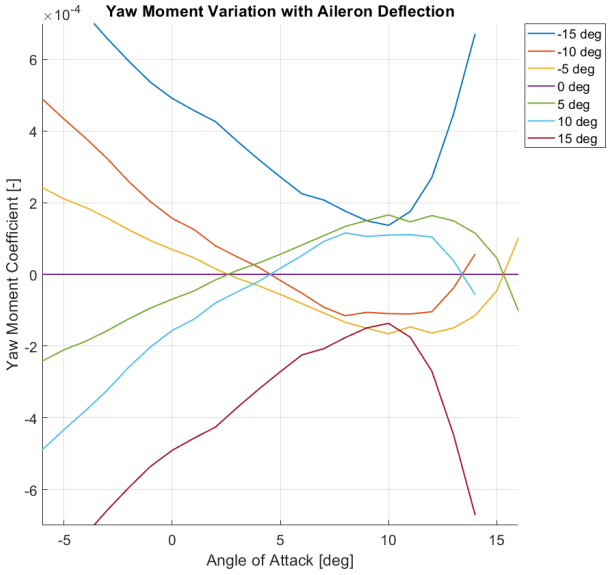

(k) Yaw Moment Coefficient with Changes in δ_a

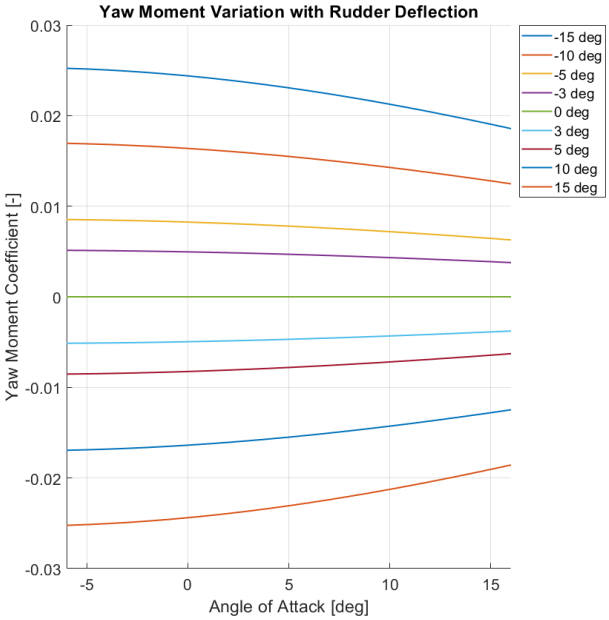

(l) Yaw Moment Coefficient with Changes in δ_r

Figure A.1: Coefficients collected from XFLR5 for various flight conditions.

B Matlab Code

```
clear

%% Ranges
alpha = -6:1:16;
beta = -10:2.5:10;

delev = [-15 -10 -5 -3 0 3 5 10 15];
daileron = [-15 -10 -5 0 5 10 15];
drudder = [-15 -10 -5 -3 0 3 5 10 15];

%% Lift

CL = readmatrix('CL_alpha.csv', 'Range', 'B:J');
CL_datum = CL(:,1);
CL = [CL(:,2:5) CL(:,1) CL(:,6:end)];
dCL_elev = CL - CL_datum;

%% Drag

CD = readmatrix('CD_alpha.csv', 'Range', 'B:J');
CD_datum = CD(:,1);
CD = [CD(:,2:5) CD(:,1) CD(:,6:end)];
dCD_elev = CD - CD_datum;

%% Pitching moment

Cm = readmatrix('Cm_alpha.csv', 'Range', 'B:J');
Cm_datum = Cm(:,1);
Cm = [Cm(:,2:5) Cm(:,1) Cm(:,6:end)];
dCm_elev = Cm - Cm_datum;

%% Heave force

% Beta
CY = readmatrix('CY_alpha_beta.csv', 'Range', 'B:J');
CY_datum = CY(:,1);
CY = [CY(:,2:5) CY(:,1) CY(:,6:end)];
dCY_beta = CY - CY_datum;

% Aileron
CY = readmatrix('CY_alpha_da.csv', 'Range', 'B:H');
CY_datum = CY(:,1);
CY = [flip(CY(:,5:end),2) CY(:,1) flip(CY(:,2:4),2)];
dCY_aileron = CY - CY_datum;

```

```
% Rudder
CY = readmatrix('CY_alpha_dr.csv', 'Range', 'B:J');
CY_datum = CY(:,1);
CY = [flip(CY(:,6:end),2) CY(:,1) flip(CY(:,2:5),2)];
dCY_rudder = CY - CY_datum;

%% Rolling moment

% Beta
Cl = readmatrix('Cl_alpha_beta.csv', 'Range', 'B:J');
Cl_datum = Cl(:,1);
Cl = [Cl(:,2:5) Cl(:,1) Cl(:,6:end)];
dCl_beta = Cl - Cl_datum;

% Aileron
Cl = readmatrix('Cl_alpha_da.csv', 'Range', 'B:H');
Cl_datum = Cl(:,1);
Cl = [flip(Cl(:,5:end),2) Cl(:,1) flip(Cl(:,2:4),2)];
dCl_aileron = Cl - Cl_datum;

% Rudder
Cl = readmatrix('Cl_alpha_dr.csv', 'Range', 'B:J');
Cl_datum = Cl(:,1);
Cl = [flip(Cl(:,6:end),2) Cl(:,1) flip(Cl(:,2:5),2)];
dCl_rudder = Cl - Cl_datum;

%% Yawing Moment

% Beta
Cn = readmatrix('Cn_alpha_beta.csv', 'Range', 'B:J');
Cn_datum = Cn(:,1);
Cn = [Cn(:,2:5) Cn(:,1) Cn(:,6:end)];
dCn_beta = Cn - Cn_datum;

% Aileron
Cn = readmatrix('Cn_alpha_da.csv', 'Range', 'B:H');
Cn_datum = Cn(:,1);
Cn = [flip(Cn(:,5:end),2) Cn(:,1) flip(Cn(:,2:4),2)];
dCn_aileron = Cn - Cn_datum;

% Rudder
Cn = readmatrix('Cn_alpha_dr.csv', 'Range', 'B:J');
Cn_datum = Cn(:,1);
Cn = [flip(Cn(:,6:end),2) Cn(:,1) flip(Cn(:,2:5),2)];
dCn_rudder = Cn - Cn_datum;
```

Member Contribution

Name	Part(s) of Project Contributed
Mikel Woo	▪ XFLR Analysis ▪ Stability and Control Derivative Calculations ▪ Holding Pattern Simulink Modeling ▪ Holding Pattern Plot Creation ▪ Report Writing and Formatting ▪ Presentation Development
Benjamin Thrun	▪ Holding Pattern Simulink Modeling ▪ Holding Pattern Writing ▪ Executive Summary ▪ Conclusion ▪ Presentation Development
Hasan Swain	
Sardor Nazarov	▪ Descent and Landing Simulink Modeling ▪ Descent and Landing Section Write-up ▪ Generation of Plots for Descent and Landing ▪ Formatting of the Report ▪ Presentation Development
Kevin Hildreth	▪ Takeoff and Climb Section Simulink Modeling ▪ Takeoff and Climb Section ▪ Report Writing ▪ Presentation Development
Zachary Bonson	▪ Takeoff and Climb Section Simulink Modeling ▪ Takeoff and Climb Section ▪ Report Writing / Plotting ▪ Aileron Control Derivative Data Gathering ▪ Report Formatting ▪ Presentation Development